Predicting Rime Ice Accretion on Airfoils

M. B. Bragg*
The Ohio State University, Columbus, Ohio

A method for predicting the droplet impingement and resulting rime ice accretion on airfoils in an incompressible, inviscid flowfield is presented. The governing equations for the water droplet trajectories are described briefly and the appropriate similarity parameters presented. Droplet impingement parameters are described for both monodisperse and arbitrary droplet size distributions. A time-stepping ice accretion process is presented where the flowfield and droplet impingement characteristics are updated periodically to model the time-dependent nature of the process. The method compares well to experimental results of both droplet impingement and rime ice shapes. The time stepping improves the accuracy of the ice shape predictions. Recommendations are given for further research.

Nomenclature

Ac = accumulation parameter, Eq. (14)
c = airfoil chord length
C_D = droplet drag coefficient
C_ℓ = airfoil lift coefficient
E = total airfoil collection efficiency, Eq. (10)
F_r = Froude number, Eq. (4)
g = gravitational acceleration constant
h = airfoil projected height
K = inertia parameter, Eq. (3)
K_0 = modified inertia parameter, Eq. (8)
ℓ = length of ice growth
LWC = liquid water content
m = mass of water droplet
R = droplet Reynolds number
r = airfoil surface radius of curvature
R_U = droplet freestream Reynolds number, Eq. (6)
S = airfoil surface arc length
T = air total temperature
t = time
U = freestream velocity
u = local flowfield velocity
x,y = horizontal and vertical coordinates
α = airfoil angle of attack
β = impingement efficiency, Eq. (9)
δ = droplet diameter
η = dimensionless droplet position
μ = absolute air viscosity
ρ = air density
ρ_{ice} = ice density
σ = droplet density
τ = nondimensional time

Introduction

AIRCRAFT structural icing occurs when an aircraft penetrates a cloud of small supercooled water droplets in flight. A portion of these droplets impinges upon the leading edges of various aircraft components resulting in the growth or accretion of ice. Rime ice occurs when the water droplets freeze on impact and form a relatively streamlined shape extending into the flow. Such an ice accretion takes place at low air temperature, low liquid water content, and low flight velocity. That is, when the energy in the system is low enough to allow the droplets to freeze immediately and not "run back." Under these circumstances, the thermodynamics of the icing process can be neglected, greatly simplifying the analysis.

The first step in predicting rime ice accretion is calculation of the droplet impingement characteristics. The first mathematical formulation of the problem was published by Taylor[1] in 1940. Here the differential equations governing droplet trajectories are formulated for the special cases of constant droplet drag coefficient and Stokes law drag. Taylor also suggested a scheme for a numerical solution of the equations which was performed by Glauret.[2] Glauret extended Taylor's formulation to include the prediction of the local mass flux on the surface and the total collection efficiency.

In 1946, Langmuir and Blodgett[3] published an excellent analytical study of the droplet impingement problem. After formulating the problem, including a more accurate droplet drag model, they performed numerous calculations on a differential analyzer. To simplify data presentation and the number of calculations required, Langmuir and Blodgett introduced the modified inertia parameter which is still in wide use.

Using essentially this same technique, NACA, in the late 1940s and early 1950s, calculated the droplet impingement characteristics of many aircraft components. Limited by the available computational power, calculations were made for bodies where the flowfield could be calculated easily; cylinders,[4,5] spheres,[6] and Joukowski airfoils.[7,8] Brun et al.[9] extended the analysis to arbitrary airfoils by generating the flowfield using a vortex substitution method based on wind tunnel measurements. This method was used extensively by NACA researchers[10-12]; later extended by Serafini[13] to include supersonic airfoils, and Dorsch and Brun[14] to include swept wings. The calculations performed by the NACA researchers proved to be very valuable. However, they continued to be limited by the available computing power until the NACA icing program was discontinued in the late 1950s.

Since approximately 1980 analytical aircraft icing research has been under way in this country and abroad. This is due in part to the wide availability of high-speed computers, and the new requirements to provide ice protection for rotorcraft and low-powered aircraft. A few researchers are involved in this development of second-generation droplet impingement codes—in Canada, Lozowski and Oleskiw,[15] Cansdale[16] in England, and Bragg et al.[17,18] in the United States. All of these studies have been conducted primarily on airfoils, as in the more recent work of Frost et al.[19] In addition, a three-

Received Nov. 2, 1983; revision received March 23, 1984.

*Assistant Professor, Department of Aeronautical and Astronautical Engineering. Member AIAA.

dimensional droplet impingement computer code is under development by Norment.[20]

The research reported herein is a refinement of the early work on this method reported by the author in 1981.[17,18] Much experience has been gained with the computer programs and several refinements have been made. The method outlined here is for rime ice only and does not address glaze ice, which often results in a more severe aerodynamic penalty. Glaze ice accretions occur due to the run back and can be predicted only by including the thermodynamics of the process. The droplet impingement method described herein is, however, applicable to the glaze ice case. This method for predicting the droplet impingement characteristics of airfoils and the resulting rime ice accretion is the first step in a complete prediction of ice accretion and the resulting airfoil performance degradation currently under way.

Analytical Method

This section presents the theoretical method for predicting the growth of rime ice on airfoils, or any other two-dimensional body. First, the equations are presented for the trajectory of a single droplet in the presence of an airfoil. Then, this can be combined to calculate the droplet impingement characteristics and later the resulting rime ice shape.

Trajectory Equation

Aircraft icing occurs when supercooled water droplets impact the leading edge of an airfoil. These droplets have diameters from 10 to 50 μm and experience relative Reynolds numbers low enough to ensure that the particles remain spherical in shape.[20] Liquid water content in the cloud rarely exceeds 2.0 g/m^3 of air. For this low concentration the flow may be considered uncoupled and the influence of the drops on the flowfield ignored. Applying Newton's Second Law to a single particle

$$m\left(\frac{\mathrm{d}^2\bar{x}}{\mathrm{d}t^2}\right)=\bar{D}+m\bar{g} \tag{1}$$

where forces due to an imposed pressure gradient, the Bassett unsteady memory term, and others, are considered negligible.[21] Only viscous drag and gravity force have been retained.

Nondimensionalizing this equation with respect to the freestream velocity U and the airfoil chord c, yields

$$\ddot{\bar{\eta}}=\frac{1}{k}\left(\frac{C_DR}{24}\right)(\bar{u}-\dot{\bar{\eta}})+\frac{1}{F_r^2}\frac{\bar{g}}{g} \tag{2}$$

where the droplet drag has been expressed in terms of the drag coefficient C_D. Here $\bar{\eta}$ is the nondimensional droplet position vector and $\dot{\bar{\eta}}$ its derivative with respect to dimensionless time τ, where $\tau=Ut/c$. The inertia parameter K is a nondimensional mass and is given by

$$K=\sigma\delta^2U/18c\mu \tag{3}$$

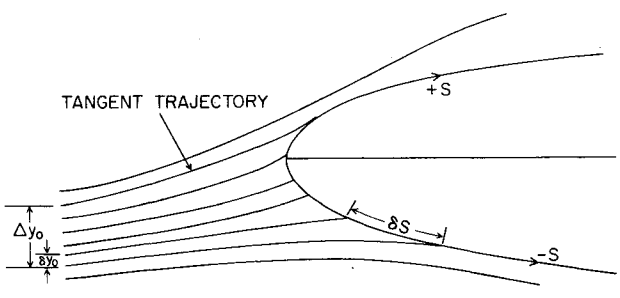

Fig. 1 Droplet trajectories used to calculate the impingement efficiency.

while the Froude number F_r is

$$F_r=U/\sqrt{cg} \tag{4}$$

Representing the droplet drag in Stokes law form, the third similarity parameter R_U appears

$$\frac{C_DR}{24}=\sum_{i=1}^{N}C_i(R_U|\bar{u}-\dot{\bar{\eta}}|)^{\gamma_i} \tag{5}$$

where

$$R_U=\rho\delta U/\mu \tag{6}$$

Now, for a given set of initial conditions on the droplet, the trajectory is determined by the values of K, F_r, and R_U for a given flowfield.

Bragg[22] has shown that Eq. (2) can be simplified using Langmuir's modified inertia parameter yielding

$$K_0\ddot{\bar{\eta}}=(\bar{u}-\dot{\bar{\eta}}) \tag{7}$$

where the gravity term has been dropped and K_0 is the average over the trajectory of the term $K/(C_DR/24)$ and can be shown to yield

$$K_0=18K[R_U^{-2/3}-\sqrt{6}R_U^{-1}\arctan(R_U^{1/2}/\sqrt{6})] \tag{8}$$

This closed-form solution for K_0 is very useful for interpreting droplet trajectory results. K_0 can now be seen as the ratio of droplet inertia to viscous drag forces. Therefore, for small values of K_0, the droplet drag dominates and the particle is very responsive to the flowfield acting almost as a flow tracer. For large K_0, the inertia dominates, and the particle is less sensitive to changes in the flowfield and diverges greatly from the flow streamlines.

To calculate the trajectory of a particle in the vicinity of an airfoil the detailed flowfield must first be determined. The dimensionless flowfield velocity $\bar{u}$ appears in the differential equation (2) and also in the expression for the droplet Reynolds number found in Eq. (5). The current method uses an inviscid, incompressible flowfield based on Woan's[23] formulation of the Theodorsen transformation. This method compares favorably to singularity methods currently in use and provides an accurate velocity anywhere in the flowfield about the airfoil.

Droplet Impingement Parameters

For a monodisperse cloud, single water droplet trajectories can be combined easily to calculate β, the impingement efficiency. The impingement efficiency is a dimensionless mass flux of material impinging at a particular point on the airfoil surface. β is nondimensionalized with respect to the mass flux in the freestream. In Fig. 1, several droplet trajectories are shown where y_0 is the initial y position of the particle and its impingement point is represented by S, the arc length measured along the surface from the leading edge. The mass of water between two trajectories a distance δy_0 apart must then be deposited over a corresponding region of the airfoil δS. It can now be seen that β can be represented in the limit as

$$\beta=\frac{\mathrm{d}y_0}{\mathrm{d}S} \tag{9}$$

where y is always measured perpendicular to the freestream. In Fig. 2, y_0 vs S has been plotted for a given case and its slope β is also shown. The maximum point on the β curve is referred to as $\beta_{\max}$ and determines the maximum ice growth approximately.

The total mass of ice accreted is proportional to the area under the β curve and is represented nondimensionally as

$$E = \Delta y_0 / h \tag{10}$$

the collection efficiency. Here h represents the maximum projected frontal height of the airfoil, a function of the angle of attack. The difference in y_0 of the two tangent trajectories is Δy_0. The tangent trajectories are those droplets which impinge upon the airfoil tangent to the surface and represent the maximum extent of icing on the upper surface S_u and on the lower surface S_L.

In an actual icing cloud the droplets are not uniform, but have some distribution of droplet diameters. In most cases this distribution can be represented adequately by the volume median droplet diameter (VMD).[18] That is, the diameter about which one-half of the mass of water in the cloud is of droplet diameter greater than the VMD and one-half less than the VMD. If representing the distribution more accurately is required, this may be done by calculating β for several droplet sizes and combining the results to get β_t and E_t as shown below[18]:

$$\beta_t(S) = \int_{\delta_{\min}}^{\delta_{\max}} \beta(\delta, S) \left(\frac{dV}{dS}\right) d\delta \tag{11}$$

$$E_t = \frac{1}{h} \int_{\delta_{\min}}^{\delta_{\max}} \Delta y_0(\delta) \left(\frac{dV}{d\delta}\right) d\delta \tag{12}$$

Here V is the dimensionless cumulative volume of water in the cloud as a function of the droplet diameter.

Ice Shape Calculation

As ice begins to accrete on an airfoil, the airfoil geometry changes. As a result the flowfield must adjust to satisfy this new boundary condition and the droplet trajectories are affected. The icing process is then seen to be a time-dependent problem where the airfoil geometry and flowfield are functions of time. An exact modeling of this system would require enormous computational resources; therefore, it is instead considered as a series of steady-state processes. This time-stepping method assumes that the droplet impingement and ice growth are constant for some period of time, after which the airfoil geometry, flowfield, and droplet impingement are updated to start another time step.

Using the information provided by the β curve, the ice shape can be predicted. Two basic assumptions are made: 1) the total mass of ice accreted during a time step is conserved, and 2) the ice grows out normal to the surface. While some researchers have proposed that the ice grows back out along the path of the droplet trajectory, this model is an approximation of the time-dependent process which leads to numerical difficulties.[18] Now for ice growth normal to the surface the ice height ℓ is given by

$$\ell + (\ell^2/2r) = Ac\beta \tag{13}$$

where r is the local surface radius of curvature. The accumulation parameter Ac represents the amount of ice in the freestream and is given by

$$Ac = \frac{U(\mathrm{LWC})\Delta t}{\rho_{\mathrm{ice}} c} \tag{14}$$

The amount and shape of the ice that accretes for a given airfoil is a function of Ac, K_0, and the airfoil angle of attack alone (noting that Reynolds and Mach number effects on the flowfield have been neglected). Note also that, in Eq. (13), the radius of curvature term tends to decrease ℓ, and thus assures the conservation of the accreted mass of water. This ice shape prediction method is discussed in more detail in Ref. 18.

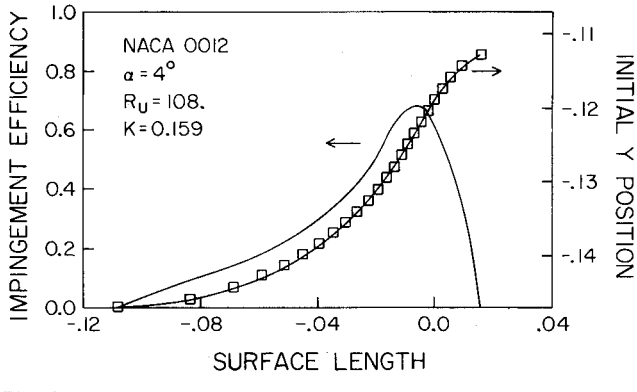

Fig. 2 Droplet trajectory data and the resulting impingement efficiency.

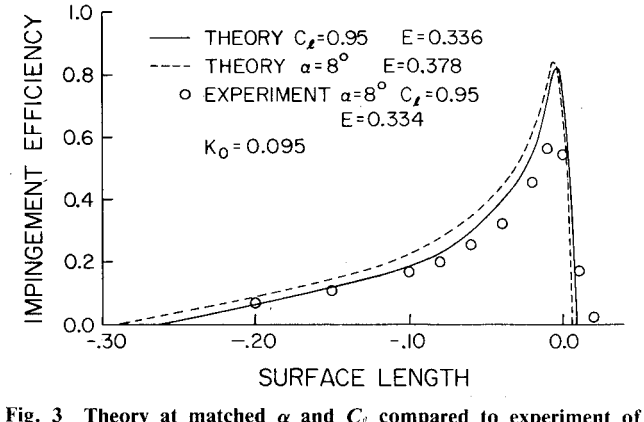

Fig. 3 Theory at matched α and C_ℓ compared to experiment of NACA TN 3839.[25]

Numerical Formulation

The numerical procedure used to predict the growth of rime ice can be separated into three basic steps, each involving one computer program. The first step is to generate and store the flowfield. This is accomplished in the present method using the Theodorsen computer program of Woan.[23] Using this flowfield, the droplet trajectories and impingement characteristics are calculated in step 2. Finally, the last step involves actually calculating the rime ice shape. In a time-stepped rime ice prediction, steps 1-3 are repeated for each step.

Droplet Trajectories

To calculate the droplet trajectory requires the numerical solution of Eq. (2). This equation is a second-order, nonlinear, ordinary differential equation. Equations of this type are generally written in component form and reduced to first order for numerical solution. This results in a system of four simultaneous first-order differential equations that can be solved by a step integration method.

The system is written in Cartesian coordinates with x parallel to the freestream and y perpendicular. Initial conditions of droplet position and velocity are required to start the solution. The droplet is assumed to be moving with the freestream velocity initially; therefore, the initial nondimensional x velocity is one and y velocity zero. It has been found that starting the droplet five chord lengths ($x_0 = -5$) in front of the airfoil is usually sufficient. The initial y coordinate, y_0, is controlled by the computer program to produce the β curve.

The differential equations are then solved using the method of Gear.[24] The method utilizes a variable step size, predictor-corrector scheme suitable for stiff systems. When compared

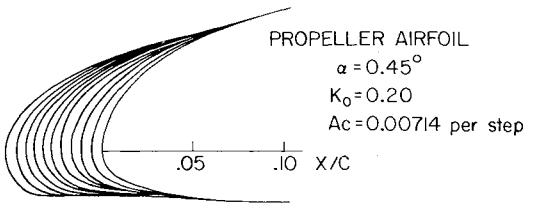

Fig. 4 Predicted rime ice growth on a propeller section.

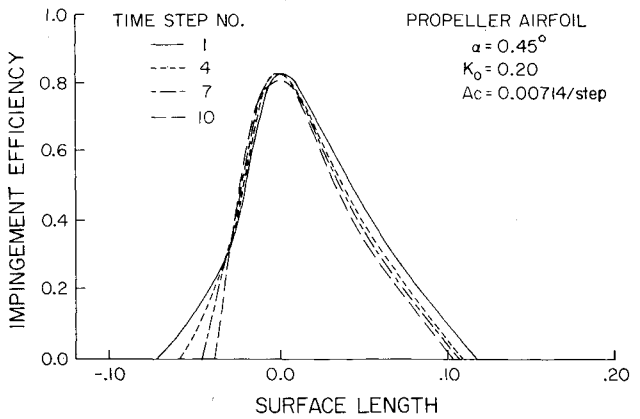

Fig. 5 Change in impingement efficiency with time during a rime ice accretion calculation.

to Adams' method on this system of equations, the stiff method reduces the computation time by at least a factor of 2. The differential equation solution requires a subroutine to evaluate the right-hand side of the system of equations represented by Eq. (2). Here the drag coefficient is calculated using the expression of Langmuir and Blodgett[3] and the gravity term is usually ignored. A trajectory calculation is terminated when a particle either impacts the surface or passes the airfoil.

Impingement Characteristics

To generate the impingement efficiency curve, a series of single droplet trajectories must be calculated. The VMD approximation replaces the distribution of droplet sizes in a cloud by the volume median drop diameter. This approximation is reasonably accurate, better for the larger droplet sizes, and saves a great deal of computer time.

The symbols in Fig. 2 are the single droplet data, y_0 vs S, for one run. The computer program searches for a droplet which hits the airfoil, then steps in even increments in y_0, up and down, until droplets have missed both above and below the airfoil. Droplet impact is determined by locally fitting a polynomial to the airfoil and trajectory. An impingement point and angle between the airfoil surface and droplet trajectory are calculated. Since the tangent trajectories are, by definition, tangent to the airfoil surface, the impingement angles are used to extrapolate to find y_0 and arc lengths for the tangent trajectories. This extrapolation is only performed after the difference between the last particle to hit, and first particle to miss the airfoil both above and below, nondimensionalized by Δy_0, is within some tolerance input by the user. This results in E being calculated to within a given error tolerance, usually 1-2% of E. The extra droplet trajectories required to satisfy this error bound are not shown in Fig. 2.

With the droplet trajectories calculated, and the tangent trajectories and E determined, the impingement efficiency curve, β, can now be predicted. β is of course just the slope of the y_0 vs S curve. This slope is determined by fitting a cubic spline through the calculated points and specifying β, i.e., the slope of the curve, equal to zero at the endpoints. The derivative of the cubic function then yields β, with the maximum, β_{max}, found analytically. For large values of K_0, droplets may impinge all the way to the trailing edge of the airfoil. In this case, β is not equal to zero for the tangent trajectory (the impingement angle is also nonzero), and the second derivative is required to be zero at this endpoint of the cubic spline.

Two comments on the numerical procedure should be made here. On airfoils where there is a change in sign of the second derivative (convex then concave surface) over a significant length of the airfoil, the β curve may not be continuous. This occurs routinely on NACA six-series airfoils due to the undercamber on the lower surface near the trailing edge. In these cases the cubic spline must be fit in pieces to give good results for β. The second comment deals with the difficulty in calculating β_{max}. For cases at high angles of attack and low K_0 the droplets impinge over only a very small region of the airfoil, sometimes as little as 1-2% chord in S. In these cases, the predicted β curve, and, of course, β_{max}, are very sensitive to the airfoil coordinates and the way in which they are fit to determine the impingement points. These cases were first run with smooth airfoil coordinates suitable for good flowfield calculations, about 120 total coordinates. It has since been found that to predict β accurately at these conditions, the coordinates must be very smooth and dense enough to have several coordinates between the limits of impingement. A smooth set of airfoil coordinates concentrated at the leading edge and lower surface is critical for good droplet impingement results.

Rime Ice Prediction

With the impingement efficiencies known as a function of S, the rime ice shape can now be predicted. Only the input β curve, the airfoil geometry, and the appropriate value of the accumulation parameter are needed. The computer program calculates the local radius of curvature of the surface and the outer normal by fitting the surface locally with a polynomial. Equation (13) is then solved for ℓ at each airfoil coordinate and the rime ice shape coordinates are calculated.

When time stepping a rime ice accretion, the whole process is merely repeated. An accumulation parameter based on the icing time per step is calculated, and an ice shape predicted for this time. The airfoil plus rime ice shape is then submitted to the flowfield code to generate a new flowfield. New droplet trajectories are run and a new β curve is calculated. Then another layer of ice is calculated and the entire procedure continues until the desired total icing time, or equivalently Ac, is reached. Numerical instability may easily be introduced if the surface radius of curvature is not handled correctly. For small values of Ac per step the r term in Eq. (13) may be negligible; if not, coordinate smoothing may be required at intervals throughout the process to prevent a rapidly growing error.

Results and Discussion

Droplet Trajectories

The droplet trajectory computer code has been compared with both experimental and other analytical results. In Table 1

Table 1 Comparison of present method to Ref. 3 for impingement characteristics on a cylinder

	Langmuir and Blodgett[3]		Present method	
	Case 1	Case 2	Case 1	Case 2
R_U	600	100	600	100
K	18.0	0.5	18.0	0.5
K_0	2.851	0.1785	2.851	0.1785
u_d	1.056	0.494	1.026	0.425
v_d	0.193	0.725	0.196	0.623
E	0.819	0.156	0.812	0.155
β_{max}	0.885	0.348	0.900	0.363
θ_m, deg	79.8	34.2	79.1	34.4

the results on a circular cylinder are compared to those of Langmuir and Blodgett.[3] Note from Table 1 that u_d and v_d are the droplet x and y velocities, respectively, on impact, and θ_m is the location of the maximum limit of impingement in degrees along the surface from the stagnation point. The comparison between the two methods is very good, especially considering the very different numerical schemes used. Comparisons of airfoils to the more recent analytical work of Refs. 15 and 16 have also been excellent.

Comparisons to the available experimental results on droplet impingement have also been made. Gelder et al.[25] used the dye-tracer technique to measure the droplet impingement efficiency on several airfoils. The present method is compared to experimental β values measured on an NACA 65_1-212 airfoil at an 8-deg angle of attack in Fig. 3. Experimental data of this type are difficult to obtain accurately due in part to problems in the calibration of the freestream mass flux. As a result, Gelder estimates that these values are good within 10%. Note also that the theoretical results shown were generated using the VMD approximation which usually slightly overpredicts β_{max} and underpredicts the limits of impingement.[18] Considering these points, the comparisons between theory and experiment are quite good, especially for the theory where C_ℓ was matched (here E was calculated using h for $\alpha = 8$ deg).

The high-angle-of-attack comparison of Fig. 3 was chosen intentionally to demonstrate one of the limitations of the present method. Other comparisons to the data of Ref. 25 at low angles of attack compare excellently at matched angles of attack. This problem at low K_0 and high angle of attack is a result of the inviscid flowfield used. Inviscid codes overpredict airfoil lift curve slopes and, of course, fail to predict the nonlinear effects near maximum lift. At low K_0 the drag force on a droplet dominates the inertia and the droplet is very sensitive to the flowfield. At large angles of attack, the airfoil circulation is an important component of the flowfield and is overpredicted by the inviscid flowfield. Therefore, at low K_0 and high angle of attack, droplet impingement characteristics are best predicted by matching airfoil C_ℓ and not angle of attack, with the impingement limits S_u and S_L being the most sensitive. At high K_0, the opposite is true since droplet inertia dominates and maintaining the proper airfoil geometry is more important than the flowfield calculations.

It is important to note that even with the error described above, the method used at matched α provides acceptable results in most cases.

Time-Stepped Ice Accretion

Using the time-stepping procedure to predict rime ice growth, several general trends appear. In Fig. 4, a time-stepped ice accretion is shown for a typical propeller airfoil at 0.45-deg angle of attack and a K_0 of 0.20. Here 10 steps were taken with each representing an Ac of 0.00714. This icing case is very severe, with the ice extending forward approximately 5% chord.

In Fig. 5, the β curves from the first, fourth, seventh, and tenth time steps are shown. Using this figure and referring also to Fig. 4, the change in the impingement characteristics and ice growth with time can be seen as summarized in Table 2. With time, the area under the β curves is decreasing. This means that the total collection efficiency, E, and the total mass accreted per step is decreasing with time. From Table 2, the decrease in E from step 1 to 10 is seen to be over 10%. While this example is fairly typical, the amount of change in E is large here and depends upon the droplet conditions and airfoil geometry. Changes in E for the various cases run to date range from almost no change to large decreases in E with time.

The maximum impingement efficiency β_{max} decreases slightly with time in the present example. β_{max} is a strong function of the leading-edge radius of the airfoil and will change inversely with changes in the radius. These changes in the leading-edge radius, and, therefore, β_{max}, are usually small, but β_{max} in general can either increase or decrease depending on the conditions.

The changes in the limits of impingement, S_u and S_L, are very significant. The values in Table 2 are measured from the leading edge of the airfoil, or airfoil plus ice shape for steps 2 on. As can be seen in Fig. 5, the limits move forward a great deal with respect to the original airfoil. For this case, Table 2 shows that S_u and S_L both decrease in absolute magnitude even with respect to the changing leading-edge point. This moving forward of the limits is a general effect that causes the ice accretion to be very thin near the limits where ice is accreted for only a short period of time. Thus, as the ice grows, the actual area over which water is impinging shrinks, or at best stays constant, but does not appear to grow as the surface area of the ice grows.

These more general comments demonstrate how important modeling the time-dependent effects on the ice accretion are. This can be seen clearly in Fig. 6, where the method is compared to an experimental shape. The measured ice shape was accreted in the NASA Lewis Icing Research Tunnel on a modified NACA 64-215 airfoil at an angle of attack of 0.7 deg.[17] The 1.613-m chord airfoil was tested at a speed of 175 m/s, a liquid water content of 0.80 g/m^3, and a -15°C total air temperature. The droplet size was 15 μm VMD, and the total icing time was 15 min. The modified inertia parameter for this case is 0.036 and the total Ac is 0.04.

In Fig. 6, the experimental rime ice shape is compared to the theory with and without time stepping. In the case without time stepping, the initial β curve is used to predict the entire 15-min ice accretion. This, of course, ignores the change in ice growth characteristics with time. The time-stepped prediction uses three 5-min steps to model the ice accretion. Here the comparison to the measured shape is excellent. The time stepping showed that β_{max} increases, while E and the maximum limits of impingement decrease with time. This is seen in the ice shape as an increased growth rate at the leading edge and reduced ice accretion near the limits of impingement compared to the case without time stepping. All of these effects improve the accuracy of the prediction. It is clearly

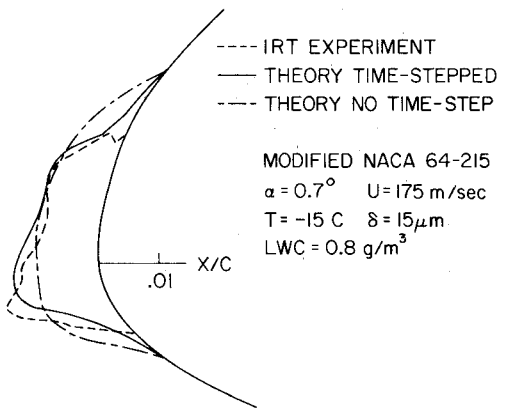

Fig. 6 Theoretical rime ice shape compared to experiment for the modified NACA 64-215 airfoil.

Table 2 Time-stepped icing parameters

Time step	E	β_{max}	S_u	S_L
1	0.539	0.835	0.120	−0.0702
4	0.499	0.833	0.110	−0.0593
7	0.468	0.835	0.106	−0.0438
10	0.448	0.815	0.104	−0.0376

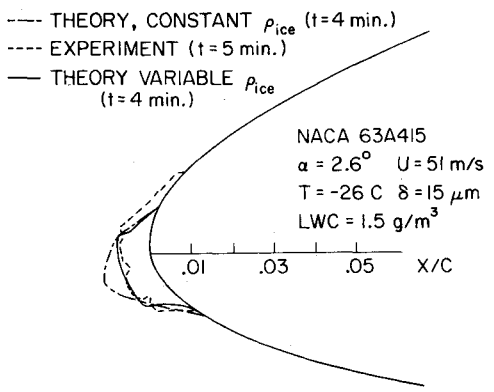

Fig. 7 Constant and variable ice density models compared to a measured rime ice shape.

seen from this example that, to accurately predict the growth of rime ice on airfoils, the time-dependent nature of the process must be modeled.

Continued use of this method to predict rime ice shapes has demonstrated that, while the mass of ice accreted always compared well, the actual ice shape predictions were more accurate at the higher temperatures than at the very low temperatures. At first, this was difficult to understand since as the temperature decreases the droplets are more likely to freeze on impact and the dry ice accretion model should become a better representation of the real physics. The problem was found to be in the assumed density of the ice. Tests conducted in the NASA Icing Research Tunnel at $-26°C$ found rime ice average densities of 0.42 and 0.534 g/cm^3 at two slightly different conditions.[26] These are far from the 0.75 to 0.90 g/cm^3 often quoted in the literature.

Not only was the density low, but it varied with position from the maximum growth point. The ice near the maximum growth point was clear, high-density ice similar to that in a glaze accretion. Further away, the ice was more opaque and was a feather-like structure (rime feathers) where small layers or fingers of ice are separated by a region of air causing an effective low-density ice. This is in contrast to the higher temperatures, $-15°C$, such as in Fig. 6, where most of the ice is of the clear, high-density type, but the temperature is still low enough to prevent excessive run back.

Macklin[27] presented a model for the ice density on a rotating cylinder as a function of the droplet impingement and thermodynamic variables. His experimental data show that ice density increases with increasing velocity, surface temperature, droplet size, and mass flux of water striking the cylinder. The Macklin equation for a rotating cylinder cannot be applied directly to an airfoil, and since a modified Macklin model would entail more thermodynamic information than exists in the present model, a simple scheme based only on β is used.

In Fig. 7, an experimental ice shape is compared to the time-stepped theory with and without variable ice density. An NACA 63A415 airfoil model of 1.37-m chord was tested at $\alpha=2.6$ deg, $U=51$ m/s, $T=-26°C$, $\delta=15$ μm, and an icing time of 5 min. The ice density was assumed to vary with β as

$$\sigma_{ice} = c_1 + c_2\beta^n$$

The constant n was chosen such that the average ice density was the measured value of 0.421 g/cm^3. c_1 and c_2 were calculated based on an assumed minimum density of 0.2 g/cm^3 at $\beta=0$ and a maximum of 0.7 g/cm^3 at β_{max}. The variable ice density theory compares very well to the measured shape using a theoretical ice accretion time of 4 min. This represents a change in the accumulation parameter on the same order as the experimental error in Ac due to the measurement of LWC, δ, ρ_{ice}, etc.

This variable ice density model was intended as a numerical experiment, and not a rigorous modification to the rime ice accretion theory. It does demonstrate, however, that at low temperatures the variations in ice density must be considered to predict rime ice shapes accurately. Also note that an accurate value of the ice density is critical in determining the overall size of the ice accretion. If, as in the case of Fig. 7, a more typical value of 0.8 g/cm^3 has been used for the ice density, the predicted ice shape would have been approximately one-half as large.

Summary

A method to predict the rime ice accretion on airfoils has been presented. The equations governing the trajectory of a single water droplet were derived and the proper scaling presented. The important droplet impingement parameters are presented for a monodisperse cloud and equations are presented to expand the analysis to an arbitrary distribution of particle sizes. A computer program has been written to solve for the droplet trajectories and impingement parameters. A step integration method is used to solve the system of equations where the flowfield is provided for the incompressible, inviscid case. To predict the rime ice shape, a time-stepping method is used where the flowfield and droplet impingement characteristics are updated periodically. Comparisons are made to measured droplet impingement results and rime ice shapes. The method compares well to both types of experimental results and the ice shape comparisons demonstrate the improved accuracy with the time-stepping method.

In the context of the comparisons of the theory to experiment a few suggestions were made as to ways the theory could be improved or made more general. While the present theory provides good predictions as shown by experiment, listed below are recommendations to improve the method further.

1) Matching the exact lift coefficient for a given angle of attack assures the correct flowfield for a given airfoil geometry. This has been shown to be important for droplet impingement at low K_0 and high angle of attack. Therefore, an improvement to the present method would be to include viscous effects in the flowfield code by adding a boundary-layer calculation and updating the potential flow using the displacement surface.

2) The method described herein is for incompressible flow only. A compressible version has been developed but no experimental droplet impingement data are available to validate the theory. This type of experimental data is needed before such a method can be used extensively.

3) A method to predict ice density for the low-temperature rime ice accretions is needed. While ice density is not as great a problem for glaze ice predictions, it does impact the accuracy of the present method's rime ice predictions under some conditions.

4) The current time-stepping method has been shown to improve rime ice predictions significantly. For glaze ice prediction where the ice shape changes the flowfield drastically, the time effects are anticipated to be even larger. The current method could be expanded to include a thermodynamic model and predict the time-dependent accretion of glaze ice.

Acknowledgments

This work was supported in part by NASA Lewis Research Center under Grant NAG 3-28. The author would like to thank Dr. R. J. Shaw of NASA Lewis for his support and helpful suggestions throughout the course of this research.

References

[1] Taylor, G. I., "Notes on Possible Equipment and Technique for Experiments on Icing on Aircraft," British Aeronautical Research Council, R&M No. 2024, Jan. 1940.

[2]Glauret, M., "A Method of Constructing the Path of Raindrops of Different Diameters Moving in the Neighbourhood of (1) a Circular Cylinder, (2) an Airfoil, Placed in a Uniform Stream of Air; and a Determination of the Rate of Deposit of the Drops on the Surface and the Percentage of Drops Caught," British Aeronautical Research Council, R&M No. 2025, Nov. 1940.

[3]Langmuir, I. and Blodgett, K. B., "A Mathematical Investigation of Water Droplet Trajectories," Army Air Forces, Tech. Rept. 5418, Feb. 1946.

[4]Brun, R. J., Serafini, J. S., and Gallagher, H. M., "Impingement of Cloud Droplets on Aerodynamic Bodies as Affected by Compressibility of Air Flow Around the Body," NACA TN 2903, March 1953.

[5]Brun, R. J. and Mergler, H. W., "Impingement of Water Droplets on a Cylinder in an Incompressible Flow Field and Evaluation of Rotating Multicylinder Method for Measurement of Droplet-Size Distribution, Volume-Median Droplet Size, and Liquid-Water Content in Clouds," NACA TN 2904, March 1953.

[6]Dorsch, R. G., Saper, P. G., and Kadow, C. F., "Impingement of Water Droplets on a Sphere," NACA TN 3587, Nov. 1955.

[7]Bergrun, N. R., "A Method for Numerically Calculating the Area and Distribution of Water Impingement on the Leading Edge of an Airfoil in a Cloud," NACA TN 1397, Aug. 1947.

[8]Brun, R. J. and Vogt, D. E., "Impingement of Cloud Droplets on 36.5-Percent-Thick Joukowski Airfoil at Zero Angle of Attack and Discussion of Use as Cloud Measuring Instrument in Dye-Tracer Technique," NACA TN 4035, Sept. 1957.

[9]Brun, R. J., Gallagher, H. M., and Vogt, D. E., "Impingement of Water Droplets on NACA 65-208 and 65-212 Airfoils at Four Angles of Attack," NACA TN 2952, May 1953.

[10]Brun, R. J., Gallagher, H. M., and Vogt, D. E., "Impingement of Water Droplets on NACA 65A004 Airfoil and Effect of Change in Airfoil Thickness from 12 to 4 Percent at 4 Angles of Attack," NACA TN 3047, Nov. 1953.

[11]Brun, R. J., Gallagher, H. M., and Vogt, D. E., "Impingement of Water Droplets on NACA 65A004 Airfoil at 8° Angle of Attack," NACA TN 3155, July 1954.

[12]Brun, R. J. and Vogt, D. E., "Impingement of Water Droplets on NACA 65A004 Airfoil at 0 Angle of Attack," NACA TN 3586, Nov. 1955.

[13]Serafini, J. S., "Impingement of Water Droplets on Wedges and Diamond Airfoils at Supersonic Speeds," NACA TN 2971, July 1953.

[14]Dorsch, R. G. and Brun, R. J., "A Method for Determining Cloud Droplet Impingement on Swept Wings," NACA TN 2931, April 1953.

[15]Lozowski, E. P. and Oleskiw, M. M., "Computer Simulation of Airfoil Icing Without Runback," AIAA Paper 81-0402, Jan. 1981.

[16]Cansdale, J. T. and Gent, R. W., "Ice Accretion on Aerofoils in Two-Dimensional Compressible Flow—A Theoretical Model," RAE Technical Rept. 82128, 198

[17]Bragg, M. B., Gregorek, G. M., and Shaw, R. J., "An Analytical Approach to Airfoil Icing," AIAA Paper 81-0403, Jan. 1981.

[18]Bragg, M. B., "Rime Ice Accretion and Its Effect on Airfoil Performance," Ph.D. Dissertation, The Ohio State University, Columbus, Ohio, 1981; also, NASA CR 165599, 1982.

[19]Frost, W., Chang, H. P., and Kimble, K. R., "Particle Trajectory Computer Program for Icing Analysis," Final Report for NASA Lewis Research Center under Contract NAS3-22448 by FWG Associates Inc., April 1982.

[20]Norment, H. G., "Calculation of Water Drop Trajectories to and About Arbitrary Three-Dimensional Bodies in Potential Airflow," NASA CR 3291, Aug. 1980.

[21]Rudinger, G., "Flow of Solid Particles in Gases," AGARDograph No. 222, 1967, pp. 55-86.

[22]Bragg, M. B., "A Similarity Analysis of the Droplet Trajectory Equation," *AIAA Journal*, Vol. 20, Dec. 1982, pp. 1681-1686.

[23]Woan, C. J., "Fortran Programs for Calculating the Incompressible Potential Flow About a Single Element Airfoil Using Conformal Mapping," Aeronautical and Astronautical Research Lab., The Ohio State University, Columbus, Ohio, TR AARL 80-02, Jan. 1980.

[24]Gear, C. W., "DIFSUB for Solution of Ordinary Differential Equations," *Communications of the Association for Computing Machinery*, Vol. 14, March 1971, pp. 185-190.

[25]Gelder, T. F., Smyers, W. H. Jr., and Von Glahn, U. H., "Experimental Droplet Impingement on Several Two-Dimensional Airfoils with Thickness Ratios of 6 to 16 Percent," NACA TN 3839, Dec. 1955.

[26]Bragg, M. B., Gregorek, G. M., and Shaw, R. J., "Wind Tunnel Investigation of Airfoil Performance Degradation Due to Icing," AIAA Paper 82-0582, March 1982.

[27]Macklin, W. C., "The Density and Structure of Ice Formed by Accretion," *Royal Meteorological Society Quarterly Journal*, Vol. 88, No. 375, Jan. 1962, pp. 30-50.